$\{\beta\}$ and $\{\alpha\}$ can be varied independently for each element. The stationary conditions of Π [Eq. (17)] with respect to these variables are

$$[H] \cdot \{\beta\} + [W] \cdot \{\alpha\} - [G] \cdot \{q\} = 0 \qquad (21)$$

$$[W]^t \cdot \{\beta\} + \{D\} = 0 \qquad (22)$$

The macroscopic equilibrium equations [Eq. (4)] are present in Eq. (22). Eqs. (21) and (22), being of the same mathematical form as those derived when stress boundary conditions are systematically enforced in hybrid models, are solved as described in detail in Ref. 7. Eliminating as many β's as possible from Eq. (22), we have

$$\{\beta\} = [R_1] \cdot \{\beta_r\} + [R_2] \cdot \{D\} \qquad (23)$$

where $\{\beta_r\}$ is a subset of $\{\beta\}$, its number being equal to that of $\{\beta\}$ minus the rank of $[W]$. The reduction matrices $[R_1]$ and $[R_2]$ are derived from $[W]^t$. Substituting Eq. (23) in Eq. (21), $\{\alpha\}$ and $\{\beta_r\}$ are expressed as a function of $\{q\}$. Substituting in Eq. (17), we have

$$\Pi = -\sum_n (\tfrac{1}{2} \cdot \lfloor q \rfloor \cdot [k] \cdot \{q\} - \lfloor \bar{Q} \rfloor \cdot \{q\} + \text{const}) \qquad (24)$$

whereby

$$[H_r] = [R_1]^t \cdot [H] \cdot [R_1] \qquad (25)$$

$$[k] = [G]^t \cdot [R_1] \cdot [H_r]^{-1} \cdot [R_1]^t \cdot [G] \qquad (26)$$

$$\{\bar{Q}\} = \{S\} + [G]^t \cdot ([R_1] \cdot [H_r]^{-1} \cdot [R_1]^t \cdot [H] - [I]) \cdot [R_2] \cdot \{D\} \qquad (27)$$

$[k]$ and $\{\bar{Q}\}$ are the stiffness matrix and the generalized load vector, respectively. Assembling all elements and enforcing the geometric boundary conditions, the final system of equations of the standard displacement method is determined.

More terms than those corresponding to the rigid-body motion can be chosen in Eq. (7), each leading to an additional equilibrium equation in Eq. (22). When the total number of α's is equal to the number of β's minus the number of coefficients of the corresponding stress assumption (of the same degree) that satisfies the differential equations of equilibrium exactly, then the latter are enforced. Additional α's would lead to linear dependencies in $[W]^t$. To guarantee that the same linear dependencies would arise in $\{D\}$, $\{\bar{F}_i\}$ must not vary with a polynomial of a higher degree than $\{\sigma_{ij}\}$. The same also holds for the equilibrium and standard hybrid models. For instance, if, for a plane stress problem, $\{\sigma_{ij}\}$ is assumed as a complete quadratic polynomial, $\{\beta\}$ will have 18 coefficients. Enforcing macroscopic equilibrium, the number of β_r's will be 15. If $\{u_i\}$ varies linearly, the number of β_r's is reduced to 12. The resulting stresses then satisfy the equilibrium equations exactly. Any quadratic term in $\{u_i\}$ would have no effect on the final result. $\{\bar{F}_i\}$ can vary as a polynomial of up to the first degree.

Many of the characteristics of the equilibrium and standard hybrid models are of course found in the corresponding generalized hybrid models. The criteria to avoid kinematical deformation modes are the same; just the expansion of $\{\sigma_{ij}\}$ given by $\{\beta_r\}$ has to be taken into consideration [Eqs. (6), (23)]. Increasing the number of α's and q's reduces the error in equilibrium and thus makes the model more flexible, while choosing a larger number of β's, reducing the error in compatability, makes the model more rigid. The alternate hybrid model is bounded from below by the extended hybrid model with the same σ_{ij} and from above by the equilibrium model using a polynomial of the same degree. The extended hybrid model is bounded from below by a compatible displacement model with the same $\tilde{u}_i$ and from above by the standard hybrid model with a polynomial for the σ_{ij} of the same degree and the same $\tilde{u}_i$. [As the convergence of the equilibrium, standard hybrid and displacement model has been proven,[3] the generalized hybrid models will also converge, but in general not monotonically, as Eq. (5) is not a minimum principle.]

As the number of β_r's of a polynomial of high degree in the alternate hybrid model satisfying macroscopic equilibrium only is larger than the number of stress coefficients in the corresponding equilibrium model, it should be possible to enforce, at least

in certain points, continuity of all stresses.[8] This is formally achieved by including the stresses not acting on the boundary in $\{T_i\}$ of Eq. (10). For the generalized hybrid models, the shear forces in plate problems can be assumed independently of the moments [Eq. (6)]. In this case, transverse shear deformability has to be included [Eq. (18)]; independent expansions for the displacements and the rotations must be chosen. If the stress-displacement relations in Eq. (2) are chosen to be satisfied exactly, $\{\sigma_{ij}\}$ is expressed as a function of $\{\alpha\}$ [Eq. (6)]. Integrating the first integral of Eq. (5) by parts for this assumption, the (negative) functional of the hybrid displacement model of Ref. 9 is derived, if in the latter $\{T_i\}$ is determined from $\{u_i\}$. For this special case, the hybrid displacement model and the extended hybrid (stress) model will give identical results. Finally, it is also possible to apply the procedure described in this note to the hybrid stress model of Ref. 10.

References

[1] Fraeijs de Veubeke, B., "Displacement and Equilibrium Models in the Finite-Element Method," *Stress Analysis*, edited by O. C. Zienkiewicz and G. S. Holister, Wiley, New York, 1965, Chap. 9.

[2] Pian, T. H. H., "Derivation of Element-Stiffness Matrices by Assumed Stress Distributions," *AIAA Journal*, Vol. 2, No. 7, July 1964, pp. 1333–1336.

[3] Pian, T. H. H. and Tong, P., "Basis of Finite-Element Methods for Solid Continua," *International Journal for Numerical Methods in Engineering*, Vol. 1, No. 1, 1969, pp. 3–28.

[4] Washizu, K., *Variational Methods in Elasticity and Plasticity*, Pergamon Press, New York, 1968, Chap. 2.

[5] Washizu, K., "Some Remarks on Basic Theory for Finite-Element Method," *Recent Advances in Matrix Methods of Structural Analysis and Design*, edited by R. H. Gallagher, Y. Yamada, and J. Tinsley Oden, University of Alabama Press, Birmingham, Ala., 1971, pp. 25–48.

[6] Prager, W., "Variational Principles for Linear Elastostatics for Discontinuous Displacements, Strains and Stresses," *Recent Progress in Applied Mechanics: The Folke Odqvist Volume*, edited by B. Broberg, J. Hult, and F. Niordson, Almqvist & Wiksell, Stockholm, 1967, pp. 463–474.

[7] Wolf, J. P., "Systematic Enforcement of Stress Boundary Conditions in the Assumed Stress Hybrid Model Based on the Deformation Method," Paper M6/10, *Proceedings of the First International Conference on Structural Mechanics in Reactor Technology*, Sept. 1971, Commission of the European Communities, Brussels, pp. 463–483.

[8] Wolf, J. P., "Structural Averaging of Stresses in the Hybrid Stress Model," *AIAA Journal*, Vol. 10, No. 6, June 1972, pp. 843–845.

[9] Tong, P., "New Displacement Hybrid Finite-Element Models for Solid Continua," *International Journal for Numerical Methods in Engineering*, Vol. 2, No. 1, 1970, pp. 73–83.

[10] Atluri, S., "A New Assumed Stress Hybrid Finite-Element Model for Solid Continua," *AIAA Journal*, Vol. 9, No. 8, Aug. 1971, pp. 1647–1649.

High-Damping Measurements and a Preliminary Evaluation of an Equation for Constrained-Layer Damping

MIIN-JENG YAN* AND E. H. DOWELL†
Princeton University, Princeton, N.J.

Nomenclature

A_{io} = area moment of the ith layer about the $z = 0$ plane
D = modulus associated with plate and equal to $E/(1-v^2)$

$G_2{}^*(\omega)$ = complex shear modulus for the intermediate viscoelastic layer

h = thickness

I_{io} = area moment of inertia of the ith layer about the $z = 0$ plane

w = transverse displacement function of the plate or beam

α, β, γ = shear, stiffness and density parameters, respectively

ρ = density

∇^2, ∇^4 = harmonic and biharmonic operators

ω = circular frequency

$(\tilde{\ })_i$ = ratio of a quantity of the ith layer to the same quantity of the first layer

$(\ )_i$ = pertaining to the ith layer of the sandwich

Fig. 2   The spectrum of a simply-supported constrained-layer damped sandwich beam.

Introduction

FOR constrained-layer damping of sandwich structures a single equation of motion describing the lateral displacements w of the plate or beam has been derived by several investigators.[1-3] However, the simplest form which retains sufficient accuracy for applications has been derived by Yan and Dowell[4,5] as

$$-\omega^2\gamma\rho_1 h_1 w + \alpha\frac{D_1 A_{10}}{G_2{}^*(\omega)}\omega^2\gamma\rho_1 h_1 \nabla^2 w + \beta D_1 I_{10}\nabla^4 w = 0 \quad (1)$$

where α, β, and γ are pure constants defined as follows:

$$\alpha \equiv \frac{\tilde{h}_2}{1+\tilde{h}_2+\tilde{h}_3}\left[\frac{\tilde{D}_3(\tilde{A}_{30}-\tilde{h}_3)}{1+\tilde{D}_3\tilde{h}_3}\right]$$

$$\beta \equiv 1+\tilde{D}_3\tilde{I}_{30} - \frac{(1+\tilde{D}_3\tilde{A}_{30})^2 A_{10}{}^2}{(1+\tilde{D}_3\tilde{h}_3)I_{10}h_1}$$

$$\gamma \equiv 1+\tilde{\rho}_2\tilde{h}_2+\tilde{\rho}_3\tilde{h}_3$$

The first term of Eq. (1) is associated with the kinetic energy, the second mainly the dissipative energy and the third the potential strain energy of the harmonic motion of a plate or beam. (In the beam case D_i should be changed to E_i.) A preliminary experimental evaluation of this equation has been made by the classical half-power damping measurement. The inherent inaccuracy of this method as well as the decay and hysteretic loop methods for constrained-layer damping measurements will also be discussed.

Inaccuracy of Various Damping Measurements

For high constrained-layer damping almost all of the usual methods of damping measurements offer difficulties in data interpretation. They need to be modified before they can be applied to measure such a highly damped continuous system. For example, the logarithmatic decrement or decay rate method is very powerful and accurate for a lightly damped system.
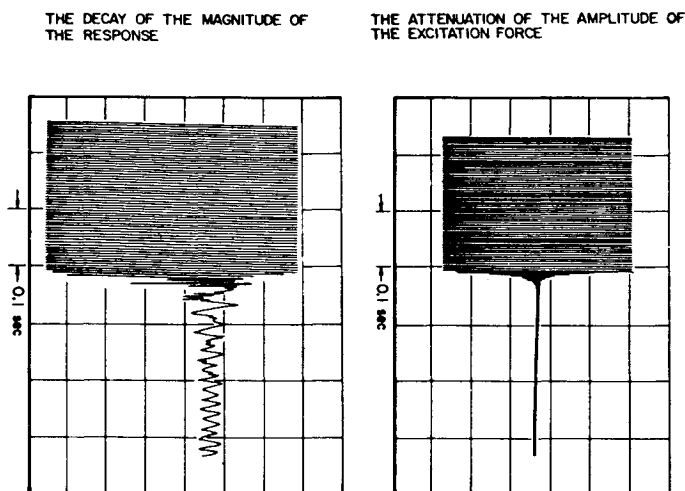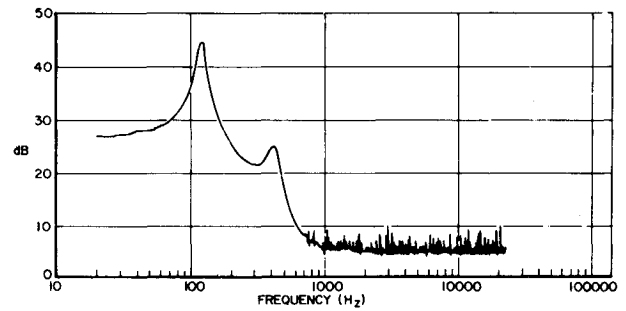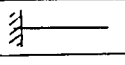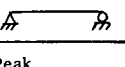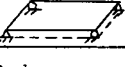
Yet for highly damped system there are difficulties. Firstly, the way the excitation is cut off affects the response, and thus, the measurement to a significant degree. There are two ways to cut off the steady sinusoidal excitations. One is by gradual attenuation of the excitation as shown in the upper figure of Fig. 1. The steady sinusoidal excitation is phase out in about 0.02 sec. Only if the response decay time is long compared with this phase-out time is this logarithmatic decrement measurement meaningful. However, the response of the constrained-layer damping is such that the decay time of the response is about the same time as the phasing-out time as shown in the lower figure of Fig. 1. Moreover, the shape of the response decay envelope in this figure prevents an accurate decay rate measurement. The signal on the right side of this figure is the noise. The other cutoff technique is a sudden disruption of the excitation. This is not desirable either, because the sudden discontinuity produces a special excitation signal and the response decays in only a few cycles as almost the same way as in Fig. 1. The response signal to this excitation disruption is even more violent than that shown in Fig. 1. Secondly, even if this cutoff technique can be improved, the discrepancy between the response and actual sinusoidal curve has to be seriously considered. For during cutoff the excitation signal is no longer purely steady sinusoidal. This discrepancy is quite significant since the response signal will decay in only few cycles for the high damping of interest here.

The half-power method may not be accurate either. For highly damped systems the response of each individual resonance spreads over a wide frequency range about its resonance frequency. The frequency range of each resonance response may extend into the responses, or may even extend beyond the resonant frequencies, of its neighboring resonances. The total response of the linear system will be the sum of these mingled resonance responses. This will make the half-power method very difficult to apply. The actual spectrum of one of the simply-supported sandwich beams is shown in Fig. 2. The larger peak is the fundamental resonance, while the smaller peak is the second resonance. The higher frequency resonances are just slightly above the noise level; thus, they cannot be identified in this spectrum. The accuracy of the half-power damping measurement on the larger peak is low, while on the smaller peak it is completely unacceptable. This same dilemma exists for any fractional power points as well.

The hysteretic loop is a measure of the temporal-phase-angle difference between the excitation and the response. It is well defined only for one-degree-of-freedom system. For the continuous system the combination of the temporal and spatial-phase-angle differences makes this hysteretic loop very difficult to apply for high damping measurements. Detail discussion on this can be found in Ref. 5.

In view of these difficulties, an urgent need exists for a significant and meaningful entity which is related to the original definition of damping of one-degree-of-freedom spring-mass-dashpot system, which can be identified and can easily be measured for high damping, and which will yield good accuracy for each mode or the entire continuous system.

THE DECAY OF THE MAGNITUDE OF THE RESPONSE

THE ATTENUATION OF THE AMPLITUDE OF THE EXCITATION FORCE

Fig. 1   The excitation and its response of a constrained-layer damped beam.

Table 1 Resonant frequencies and damping coefficient by half-power method of the sandwich beam and plate with different boundary conditions

	ω_1 & ζ_1		ω_2 & ζ_2		ω_3 & ζ_3	
Peak Frequency	37	(40)*	222	(238)	611	(668)
Half-Power Frequency	35	38	198	240	507	664
Damping Coefficient	.041	(.039)	.095	(.092)	.128	(.095)

	ω_1 & ζ_1		ω_2 & ζ_2		ω_3 & ζ_3	
Peak Frequency	119	(113)	414	(425)	?	
Half-Power Frequency	112	126	?	451		
Damping Coefficient	.059	(.048)	.091**	(.091)		

	ω_{11} & ζ_{11}		ω_{21} & ζ_{21}		ω_{31} & ζ_{31}	
Peak Frequency	122	(126)	182	(196)	277	(309)
Half-Power Frequency	114	127	?	199	238	316
Damping Coefficient	.053	(.060)	.093**	(.073)	.141	(.091)

*Numbers in parenthesis are calculated data.
**This coefficient is based upon only the right half-power point by assuming symmetry.

Results and Discussion

The half-power method is used for this preliminary evaluation of Eq. (1) with an expected relatively high error in measured damping coefficients. The experimental procedure is standard. The harmonic excitation is varied through the frequency range of interest, the frequency response of the structure constructed, and then the peak frequency and corresponding half-power frequencies read. Details of this procedure can be found in Ref. 5. An aluminum beam, 9 in. long, 0.065 in. thick, covered with a 0.022-in. DuPont viscoelastic damping material and by an additional 0.020-in. aluminum constraining layer, subjected to simply supported and cantilever boundary conditions is considered. The measured and calculated results are shown in Table 1. In the simply supported beam case the lower half-power point of the second resonance could not be measured as is shown in Fig. 2. Data for a simply supported sandwich plate of 19.75 in. long by 9.75 in. wide with the same thickness configuration of the beam are also shown in this table.

The error between measured and calculated data with respect to the measured data for resonant frequencies is from 2% to 11% for all the resonances shown in Table 1. The experimental measurement of resonant frequencies itself is accurate within 1 Hz. Thus it is believed that Eq. (1) predicts the resonant frequencies for the sandwich beam as accurate as the classical beam equation for an uniform elastic beam.

The error between measured and calculated data with respect to the measured data in damping coefficients is from 0% to 35%. This error arises from many possible sources; however, the mingling of the resonance tails is the prevailing source in most cases. Although this damping error is relatively high, it is believed that a well-designed high damping measurement method for the constrained-layer damping could reduce the error.

Additional discussion and comparison of calculated data using the present theory with the experimental data obtained by the decay method on various sandwich configurations reported in NASA CR-742 (Ref. 6) are also given in Ref. 5. These tend to strengthen the aforementioned conclusions.

References

[1] Ross, D., Ungar, E. E., and Kerwin, E. M., Jr., "Damping of Plate Flexural Vibrations by Means of Viscoelastic Laminae," *Colloquium on Structural Damping,* ASME, New York, Dec. 1959, Sec. 3, pp. 50–87.

[2] DiTaranto, R. A., "Theory of Vibratory Bending for Elastic and Viscoelastic Layered Finite-Length Beams," *Transactions of the ASME, Journal of Applied Mechanics,* 1965, pp. 881–886.

[3] Mead, D. J. and Markus, S., "The Forced Vibration of a Three-Layer, Damped Sandwich Beam with Arbitrary Boundary Conditions," *Journal Sound Vibration,* Vol. 10, No. 2, 1969, pp. 163–175.

[4] Yan, M.-J. and Dowell, E. H., "Governing Equation for Vibrating Constrained-Layered Damping in Sandwich Plates and Beams," *Transactions of the ASME, Journal of Applied Mechanics,* Nov. 1972, to be published.

[5] Yan, M.-J., "Constrained-Layer Damping in Sandwich Beams and Plates," Ph.D. thesis, June 1972, Princeton Univ.; also AMS Rept. 1031, June 1972, Princeton Univ., Princeton, N.J.

[6] Ruzicka, J. E., Derby, T. F., Schubert, D. W., and Pepi, J. S., "Damping of Structural Composite with Viscoelastic Shear-Damping Mechanics," NASA CR-742, March 1967.

Engineering Analysis of Reattaching Shear Layer Heat Transfer

D. E. Nestler*
General Electric Company, Philadelphia, Pa.

Nomenclature

H = total enthalpy
$I_2(\eta_j)$ = Korst-Chow integral (Ref. 5)
M = Mach number
n = exponent in wall jet heat flux decay [Eq. (4)]
p = static pressure
Pr = Prandtl number
$\dot{q}$ = wall heat flux
Re = Reynolds number
St = Stanton number
T = temperature
U = velocity
X_R = recirculation distance from location of maximum heat flux (Fig. 1)
β = flow reattachment angle (Fig. 1)
Δ_D = shear layer width above dividing streamline (Fig. 1)
λ = freestream turbulence heating augmentation factor
μ = absolute viscosity
ρ = density
σ = turbulent shear layer spread parameter

Subscripts

D = dividing streamline
e = edge of boundary layer or shear layer
max = maximum
s = stagnation
w = wall
o = at compression ramp corner